

The role of the support properties in the catalytic performance of an anchored copper(II) aza-bis(oxazoline) in mesoporous silicas and their carbon replicas†

Cite this: *Catal. Sci. Technol.*, 2013, **3**, 659

Ana Rosa Silva,^{*a} Vanessa Guimarães,^a Ana Paula Carvalho^b and João Pires^b

A copper(II) chiral aza-bis(oxazoline) catalyst (CuazaBox) was anchored onto ordered mesoporous silicas and their carbon replicas. The materials were characterized by elemental analysis (C, N, H, S), ICP-AES, FTIR, XPS, thermogravimetry and isotherms of N₂ adsorption at -196 °C. The materials were tested as heterogeneous catalysts in the reaction of cyclopropanation of styrene to check the effect of porous material type on the catalytic parameters, as well as on their reutilization. Generally, the composites were more active and enantioselective in the cyclopropanation of styrene than the corresponding homogeneous phase reaction run under similar experimental conditions. The materials pH_{pzc} proved to be an important factor not only in the CuazaBox anchoring yields, but also in their catalytic performance. Less acidic surfaces (SPSi and CMK-3) yielded heterogeneous catalysts with higher styrene conversion and enantioselectivity. The materials could also be recycled with comparable enantioselectivities or generally a slight decrease in the enantioselectivity.

Received 12th September 2012,
Accepted 22nd October 2012

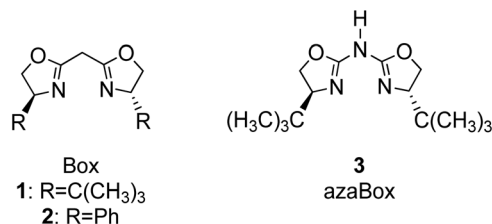
DOI: 10.1039/c2cy20638b

www.rsc.org/catalysis

1. Introduction

The synthesis of chiral cyclopropanes remains a considerable challenge, especially due to the fact that cyclopropane rings are often found in a variety of natural products and biologically active compounds.^{1,2} Therefore, it is crucial to develop useful methods for the synthesis of cyclopropanes. The catalytic asymmetric cyclopropanation of alkenes with diazoacetates has been intensively studied over the last few years by copper complexes with chiral nitrogen ligands such as bis(oxazoline) (1 and 2, Scheme 1)² and aza-bis(oxazoline) (3, Scheme 1).^{3,4} These homogeneous catalysts have also demonstrated excellent results in several other asymmetric catalytic reactions, including asymmetric aziridination,⁵ Diels–Alder,⁶ Henry reactions,⁷ etc.⁸ Chiral aza-bis(oxazoline) ligands (3) are obtained in several steps from derivatives from chiral amino alcohols.^{3,8,9}

There are different advantages associated with the choice between homogeneous and heterogeneous catalysts. Homogeneous catalysts exhibit high activity and selectivity in several organic reactions. Nevertheless, there is the possibility of



Scheme 1 Commercial bis(oxazoline) (1 and 2) and aza-bis(oxazoline) (3) chiral ligands.

product contamination due to incomplete separation of the catalyst and problems with expensive catalyst recovery are frequent.¹⁰ Heterogeneous catalysts have obvious advantages over homogeneous catalysts with respect to easy separation of the catalyst from the reaction mixture at the end of the reaction, efficient recycling, improved handling and process control, minimization of metal leaching and low cost.^{10–13} However, this type of catalysts often present limited activity and selectivity, and hence it is important to find additional value information to overcome their disadvantages and convince the organic synthesis community and industry of the advantages of heterogeneous catalysts.¹¹

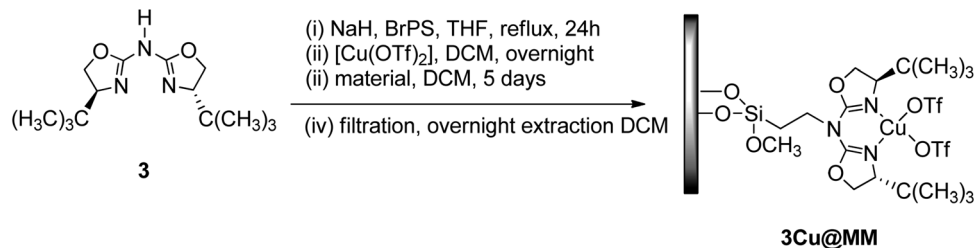
In recent years, the interest in ordered mesoporous materials has been growing due to their advantageous properties over traditional porous materials such as high dispersion of catalytic sites, resulting in a well-defined surface and uniform pore size

^a Departamento de Química, CICECO, Universidade de Aveiro, Campus Universitário de Santiago, 3810-193 Aveiro, Portugal.

E-mail: ana.rosa.silva@ua.pt; Fax: +351 234 401 470; Tel: +351 234 370 604

^b CQB, Departamento de Química e Bioquímica, Faculdade de Ciências, Universidade de Lisboa, 1749-016 Lisboa, Portugal

† Electronic supplementary information (ESI) available. See DOI: 10.1039/c2cy20638b



Scheme 2 Anchoring procedure for the copper(II) aza-bis(oxazoline) complex onto the mesoporous materials (MM).

distribution, and large specific surface area.^{14,15} Hence, these materials are recognized as being an excellent option for support of homogeneous catalysts.¹⁵

Ryoo *et al.* reported the first synthesis of ordered mesoporous carbon (OMC) CMK-3 *via* a nanocasting route using SBA-15 mesoporous silica as the template in 1999.¹⁶ This method consisted of the use of a regular rigid template (SBA-15), filled with a precursor, and posterior polymerization, carbonization and removal of the template. On the other hand, Ting *et al.* described a method that allows the one pot synthesis of mesoporous materials with different types of porous regularity.¹⁷ In this case the silica material (SPSi) and its replicate (SPC) are synthesized at the same time.^{15,17} Carbonization and removal of the silica template with HF yields mesoporous carbon, whereas heating in air leads to mesoporous silica.^{15,17}

We already reported the asymmetric cyclopropanation of styrene by copper(II) bis(oxazoline) encapsulated onto zeolites¹⁸ and anchored onto mesoporous silicas^{19,20} and carbons.²⁰ The best results were obtained using the anchored copper complex with ligand 2 (2Cu catalyst, Scheme 1) onto mesoporous silica, but generally low to moderate enantioselectivities were obtained with low recyclability.²⁰

It has been reported that in ligands 3 (Scheme 1), the presence of a nitrogen atom instead of a carbon atom at the center leads to a stronger interaction between the chiral ligand and the copper than in the case of bis(oxazoline) (Box, Scheme 1) and hence higher stability of the copper complex formed.⁴ Therefore better enantioselectivities in the asymmetric cyclopropanation of alkenes and stability upon reuse have been observed for these immobilized homogeneous catalysts onto siliceous mesocellular silica foams and organic polymers.^{3,4,21,22} At the same time, more flexibility after immobilization is obtained with these catalysts than with bis(oxazoline), 1 and 2 type ligands (Scheme 1).³

Therefore, herein, we report the anchoring of copper(II) aza-bis(oxazoline) (3) onto several unexplored mesoporous silicas (SBA-15, SPsi, HMS) and carbon materials (CMK-3, SPC), in order to evaluate the effect of the type of structure and properties of the materials on the activity, enantioselectivity and recyclability of the heterogeneous catalysts (Scheme 2).

2. Experimental section

2.1. Materials

Tetraethyl orthosilicate (TEOS, 98%), (EO)₂₀(PO)₇₀(EO)₂₀, sucrose ($\geq 99.5\%$), HF ($\geq 48\%$), 1-dodecylamine (98%),

copper(II) trifluoromethanesulfonate (copper triflate, [Cu(CF₃SO₃)₂] or [Cu(OTf)₂], 98%), (*S*)-*tert*-leucinol (98%), sodium cyanide ($\geq 97.0\%$), bromine (reagent grade), ammonia solution 2.0 M in methanol, diethyl carbonate ($\geq 98.0\%$), sodium ethoxide ($\geq 95\%$), triethylxonium tetrafluoroborate solution 1.0 M in dichloromethane, *p*-toluenesulfonic acid monohydrate ($\geq 98.5\%$), sodium hydroxide (p.a.), sodium bicarbonate (p.a.), sodium sulphate ($\geq 99.0\%$), sand (50–70 mesh particle size), triethylamine (Et₃N, $\geq 99\%$), 3-bromopropyltrimethoxysilane (BrPS, $\geq 97.0\%$), deuterated chloroform (99.8 atom% D, 0.03% (v/v) TMS), dry toluene (99.8%), dry tetrahydrofuran (THF, $\geq 99.9\%$), methanol (p.a.), styrene ($\geq 99\%$), *n*-undecane ($\geq 99\%$), ethyldiazoacetate (EDA, $\leq 15\%$ dichloromethane), phenylhydrazine (97%) and potassium bromide (FT-IR grade, $\geq 99\%$) were purchased from Aldrich and used as received. Sodium hydride (55–65%) was from Fluka. Ammonium chloride (p.a.), ethanol (p.a.) and HCl (37%) were from Panreac. H₂SO₄ (95–97%) from José Manuel Gomes dos Santos Lda. Ethyl acetate (>99.9%), *n*-hexane (95%) and dichloromethane (DCM, $\geq 99.9\%$) were from Romil. Silica gel 60 (63–200 μm) and TLC silica gel 60 F254 were from Merck.

2.2. Preparation of SBA-15

SBA-15 synthesis was based on the literature.^{23,24} About 4.0 g of the co-polymer (EO)₂₀(PO)₇₀(EO)₂₀ was dissolved in a concentrated HCl solution. Then tetraethyl orthosilicate (TEOS) was added to this solution with constant stirring. The obtained solution was stirred at 35 °C for 24 hours and subsequently heated at 100 °C for 24 hours, under static conditions. Afterwards, the solution was filtered and the filtrate was set aside for drying in air. The dried up filtrate was calcinated at 550 °C for 5 h with a ramp of 1 °C min⁻¹.

2.3. Preparation of CMK-3

The preparation of CMK-3 was based on previous works.²⁴ Briefly, solid sucrose was dissolved in a concentrated H₂SO₄ solution to which the SBA-15 sample was added under mixing. The as obtained paste was heated in an oven at 100 °C for 6 hours and subsequently at 160 °C for 6 hours. The resulted black powder was then mixed again with sucrose solution (in H₂SO₄) and reheated with a similar heating program. The obtained black powder was further carbonized, at 875 °C for 1 hour with a ramp of 10 °C min⁻¹, under vacuum. The silica template was then removed by treatment with HF acid followed by repeated washing with distilled water (until neutral pH).

The so obtained carbon (CMK-3) was then dried at 95 °C and stored in a dry place.

2.4. Preparation of SPSi and SPC in one step

In this methodology a silica-carbon composite material is firstly formed. If heated, the composite will produce a silica material (SPSi) or, if carbonized, will produce the SPC carbon. The preparation of the porous silica SPSi and the corresponding carbon replica SPC was described in detail elsewhere.¹⁵ In short, the co-polymer (EO)₂₀(PO)₇₀(EO)₂₀ was dissolved in water and a 2 M HCl solution was added under stirring. To the stirred mixture concentrated H₂SO₄, sucrose and tetraethyl-orthosilicate were added. The solution was kept at 50 °C, and stirred for 24 hours, then it was aged hydrothermally in an autoclave at 100 °C for a further 24 hours. The obtained composite was dried in an oven at 100 °C and then in a furnace at 160 °C for 6 hours. When heated in air under static conditions at 550 °C for 6 hours, the synthesized composite generated the silica sample (SPSi). The corresponding carbon sample (SPC) was formed *via* carbonization of the composite under a dry nitrogen flow at 900 °C for 12 hours, and then the silica being removed with a 40% HF. The solid was finally filtered, washed with water and ethanol, and finally dried in a oven at 70 °C.

2.5. Preparation of HMS

HMS was made according to the literature.²⁵ A solution of 10.3 mL of 1-dodecylamine in 88.1 mL of ethanol, and 88.5 mL of deionized water, was stirred for a few minutes. Then 37 mL of tetraethyl orthosilicate (TEOS) was added. The mixture was kept under stirring at room temperature for 24 hours. The white product was then filtered and washed with deionized water until the pH is neutral and then with ethanol. The final product was calcinated at 600 °C for 6 hours with a ramp of 1 °C min⁻¹.

2.6. Preparation and characterization of aza-bis(oxazoline) (3)

The synthesis of aza-bis(oxazoline) (3, Scheme 1) was performed in four steps, by adapting reported procedures.^{3,9}

Synthesis of aminoxazoline. First, aminoxazoline was synthesized; 9.38 mmol of sodium cyanide was added in small portions to a solution of 9.38 mmol of bromine in methanol (12 mL) at 0 °C. Then 8.53 mmol of (*S*)-*tert*-leucinol in methanol (2 mL) was added and the mixture was stirred at room temperature for one hour. After treatment with ammonia solution in methanol (31 mL, 2.0 M), the solvent was evaporated under reduced pressure. The residue was dissolved in an aqueous solution of NaOH (36 mL, 20% w/w) and was then extracted 5 times with 15 mL of ethyl acetate. The combined organic phases were dried with anhydrous Na₂SO₄, the solvent was evaporated under reduced pressure, and the remaining (*S*)-*tert*-leucinol was removed under reduced pressure at 60 °C for 2 days. The substance was used for the next step without further purification. White solid; yield: 0.86 g (71%); ¹H NMR (300 MHz, CDCl₃), δ/ppm: 4.19–4.25 (t, *J* = 8.8 Hz, 1 H), 4.05–4.10 (dd, *J* = 7.1 and 8.2 Hz, 1 H), 3.72–3.77 (dd, *J* = 7.1 and 9.2 Hz, 1H), 0.87 (s, 9 H); MS (ESI), *m/z*: 143.12 [M + H]⁺; FTIR, ν/cm⁻¹: 3425 s, 2954 s, 1699 vs, 1680 vs, 1649 m, 1406 m, 1011 m.

Synthesis of oxazolidinone. Secondly, oxazolidinone was synthesized; 8.53 mmol of sodium ethoxide was added to a solution of 8.53 mmol of (*S*)-*tert*-leucinol and 9.33 mmol of diethyl carbonate in ethanol (12 mL) and the mixture was refluxed for 15 hours. The solvent was evaporated under reduced pressure and then the residue was dissolved in DCM (25 mL). The solution was washed with a saturated solution of ammonium chloride (13 mL) and then the aqueous phase was extracted 2 times with DCM (13 mL). The combined organic extracts were dried with anhydrous Na₂SO₄ and the solvent evaporated under reduced pressure. Finally, the white solid was dried under vacuum for 2 days. The substance was used for the next step without further purification. Yield: 1.10 g (90%); ¹H NMR (300 MHz, CDCl₃), δ/ppm: 5.78 (s, 1H), 4.35–4.41 (t, *J* = 9.0 Hz, 1H), 4.18–4.23 (ddd, *J* = 12.6, 5.8, 1.3 Hz, 1H), 3.57–3.62 (ddd, *J* = 8.9, 5.8, 1.1 Hz, 1H), 0.91 (s, 9H); MS (ESI), *m/z*: 144.10 [M + H]⁺, 166.08 [M + Na]⁺; FTIR, ν/cm⁻¹: 3300 s, 2970 s, 1745 vs, 1720 vs, 1481 m, 1402 m, 1369 m, 1238 s, 1101 m, 1053 m, 984 m, 926 m.

Synthesis of ethoxyoxazoline. Thirdly, ethoxyoxazoline was synthesized; 10.1 mmol of a triethylxonium tetrafluoroborate solution in dichloromethane (10.1 mL, 1.0 M) was added dropwise for 30 minutes to 7.71 mmol of oxazolidinone in anhydrous DCM (16 mL) at 0 °C, in an inert atmosphere. The solution was stirred for 30 hours at room temperature, in an inert atmosphere, and then it was added to a cold saturated solution of sodium hydrogenocarbonate (32 mL). The organic phase was separated and the aqueous phase extracted 3 times with DCM (8 mL). The organic phases were dried with anhydrous sodium sulphate and then an oil was obtained after solvent evaporation under reduced pressure. The substance was used for the next step without further purification. Yield: 1.22 g (92%); ¹H NMR (300 MHz, CDCl₃), δ/ppm: 4.15–4.30 (m, 4H), 3.73–3.78 (m, 1H), 1.32–1.37 (t, *J* = 7.1 Hz, 3H), 0.88 (s, 9H); MS (ESI), *m/z*: 172.13 [M + H]⁺; FTIR, ν/cm⁻¹: 3566 m, 3386 m, 3249 m, 2966 s, 1732 vs, 1670 vs, 1537 s, 1479 m, 1406 m, 1371 m, 1263 s, 1057 s (broad), 937 m.

Synthesis of aza-bis(oxazoline) (3). Finally, aza-bis(oxazoline) was synthesized; 0.61 mmol of *p*-toluenesulfonic acid were added to 3.80 mmol of ethoxyoxazoline and 6.05 mmol of aminoxazoline in 40 mL of dry toluene and refluxed for 24 hours, in an inert atmosphere. The solvent was evaporated under reduced pressure and the crude product was purified by chromatography on silica gel using ethyl acetate/*n*-hexane 9 : 1 as the eluent to yield an oil. Colorless crystals could be obtained by recrystallization from acetone. Yield: 0.69 g (68%); ¹H NMR (300 MHz, CDCl₃), δ/ppm: 4.27–4.33 (t, *J* = 9.2 Hz, 2H), 4.12–4.17 (dd, *J* = 6.7 and 8.9 Hz, 2H), 3.78–3.84 (dd, *J* = 6.7 and 9.4 Hz, 2H), 0.90 (s, 18H); MS (ESI), *m/z*: 268.20 [M + H]⁺; FTIR, ν/cm⁻¹: 3438 m, 2958 m, 1637 s, 1585 s, 1387 m, 1092 m.

2.7. Preparation and characterization of the homogeneous catalyst (3Cu)

The copper(II) complex with ligand 3 was prepared by dissolution in DCM of equimolar quantities of [Cu(OTf)₂] (0.012 mmol) and azaBox (0.012 mmol) and stirring for 4 hours at room

temperature. The solution was filtered and upon evaporation of the solvent a green oil was obtained. FTIR, ν/cm^{-1} : 2970 m, 1728 m, 1626 s, 1261 vs, 1174 s, 1036 s, 648 s.

2.8. Anchoring of the CuzaBox (3Cu) onto the mesoporous materials

This method was adapted from a reported procedure²¹ and has three main steps: (i) functionalization of ligand **3**, (ii) coordination of copper(II) onto ligand **3** and (iii) anchoring of **3Cu** onto the surface of the material (Scheme 2). Typically, 0.112 mmol of **3** were reacted with 0.124 mmol of sodium hydride (1.1 equiv.) in 2.5 mL of dry THF and the mixture was stirred at 60 °C for 6 hours. Then, 0.112 mmol of 3-bromopropyltrimethoxysilane were added to the clear solution and further stirred overnight at 60 °C. The solvent was evaporated under reduced pressure and 15 mL of DCM were added, followed by 0.112 mmol of $[\text{Cu}(\text{OTf})_2]$. After stirring for 24 hours at room temperature, 0.50 g of mesoporous material was added to the green solution and the mixture was stirred for 5 days at room temperature. The resulting solid was filtered off, washed with DCM and then further stirred with DCM overnight, at room temperature, to remove untethered species. Finally, after filtration the solid was dried under vacuum at 60 °C for 2 days, yielding green solids in the case of the mesoporous silicas and obviously black in the case of mesoporous carbon.

3Cu@SBA-15: elemental analysis (%) N 0.51, C 3.12, H 0.90, S 0.94; ICP-AES Cu 1.0%; loading of **3** 121 $\mu\text{mol g}^{-1}$ and loading of Cu 157 $\mu\text{mol g}^{-1}$.

3Cu@CMK-3: elemental analysis (%) N 0.50, C 80.71, H 1.12, S 0.94; ICP-AES Cu 0.9%; loading of **3** 119 $\mu\text{mol g}^{-1}$ and loading of Cu 142 $\mu\text{mol g}^{-1}$.

3Cu@SPSi: elemental analysis (%) N 0.64, C 3.92, H 0.70, S 0.89; ICP-AES Cu 1.0%; loading of **3** 151 $\mu\text{mol g}^{-1}$ and loading of Cu 157 $\mu\text{mol g}^{-1}$.

3Cu@SPC: elemental analysis (%) N 0.40, C 79.95, H 0.74; ICP-AES Cu 0.57%; loading of **3** 94 $\mu\text{mol g}^{-1}$ and loading of Cu 90 $\mu\text{mol g}^{-1}$.

3Cu@HMS: elemental analysis (%) N 0.35, C 2.61, H 1.13, S 0.78; ICP-AES Cu 0.88%; loading of **3** 83 $\mu\text{mol g}^{-1}$ and loading of Cu: 138 $\mu\text{mol g}^{-1}$.

2.9. Physical and chemical methods

Elemental analysis (C, N, H and S) was performed in duplicate at Servicio de Análisis Instrumental, CACTI Vigo, Universidade de Vigo, Spain, or at Department of Chemistry of the University of Aveiro, Portugal. The copper ICP-AES was performed at "Laboratório Central de Análises" of the University of Aveiro, Portugal.

FTIR spectra of the materials were obtained as KBr pellets (2.5–3 mg of sample diluted with 200 mg of KBr or for oils a drop on the surface of a KBr pellet), in the range of 400–4000 cm^{-1} , with a FT Mattson 7000 galaxy series spectrophotometer or by ATR (mesoporous silicas) with a Bruker Tensor 27 spectrophotometer; all spectra were collected at room temperature, after drying the pellets in an oven at 75 °C overnight or the

mesoporous silicas at 100 °C for 6 hours, using a resolution of 4 cm^{-1} and 256 scans.

X-ray photoelectron spectroscopy was performed at Centro de Materiais da Universidade do Porto (Portugal), using a VG Scientific ESCALAB 200A spectrometer using non-monochromatized Mg K α radiation (1253.6 eV). All the materials were compressed into pellets prior to the XPS studies. In order to correct possible deviations caused by electric charge of the samples, the C 1s line at 285.0 eV was taken as the internal standard.

The pH measurements for determination of the pH_{pzc} (pH at which the material has a net zero surface charge) were made with a SympHony SP70P VWR pH meter. The assays were made by reverse mass titration following the method proposed by Noh and Schwarz.²⁶ Thermogravimetry was performed under air flux with a ramp of 5 °C min^{-1} in a TG-DSC apparatus, model 111 from Setaram.

Nitrogen adsorption isotherms at –196 °C were measured in an automatic apparatus (Asap 2010; Micromeritics). Before the adsorption experiments the samples were outgassed under vacuum for 2.5 h at 150 °C.

2.10. Catalysis experiments

The catalytic activity of the silica based materials, in the cyclopropanation of styrene, was tested at room temperature in batch reactors at atmospheric pressure and with constant stirring. In the experiments, typically, 2.4 mmol of styrene, 0.65 mmol of *n*-undecane, 70 mg of heterogeneous catalyst in 10.0 mL of dichloromethane and 2 μL of phenylhydrazine were used. Finally, 2.75 mmol of ethyldiazoacetate (EDA) was added to the reaction mixture over 2 hours using a syringe pump. When the addition of ethyldiazoacetate was completed, aliquots (0.05 mL) were periodically withdrawn from the reaction mixture with a hypodermic syringe, filtered through PTFE 0.2 μm syringe filters, and analyzed by GC-FID by the internal standard method. At the end of the reactions the heterogeneous catalyst was recovered by filtration, washed extensively with DCM, dried under vacuum and reused in another cycle using the same experimental procedure.

Control experiments were also performed using this experimental procedure in a homogeneous phase with **3Cu** or equimolar quantities of $[\text{Cu}(\text{OTf})_2]$ plus **3** in order to compare with the heterogeneous ones (Table 3).

The reaction mixture was analyzed by GC-FID (using the internal standard method) on a Varian 450 GC gas chromatograph equipped with a fused silica Varian Chrompack capillary column CP-Sil 8 CB Low Bleed/MS (15 m \times 0.25 mm id; 0.15 μm film thickness), using helium as a carrier gas. The enantiomeric excesses (%ee) of cyclopropanes were determined in the same chromatograph but using a fused silica Varian Chrompack capillary column CP-Chiralsil-Dex CB (25 m \times 0.15 mm i.d. \times 0.25 μm film thickness). Conditions used: 60 °C (3 min), 5 °C min^{-1} , 170 °C (2 min), 20 °C min^{-1} , 200 °C (5 min); injector temperature, 200 °C; detector temperature, 230 °C. The several chromatographic peaks were identified against commercially available samples and/or by GC-MS (Finnigan Trace).

3. Results and discussion

3.1. Materials characterization

Parent mesoporous materials. In this work three different mesoporous silicas that have never been used as supports for aza-bis(oxazoline) ligands were synthesized: SBA-15, an ordered mesoporous silica well-known and used in heterogeneous catalysis;^{10,12} SPSi, prepared by a one pot methodology described by Ting *et al.*^{15,17} and a hexagonal mesoporous silica (HMS) prepared by using a simple procedure reported by Tanev and Pinnavaia.²⁵ The analysis of the isotherms of adsorption of nitrogen at $-196\text{ }^{\circ}\text{C}$ (Fig. 1) shows that SBA-15 and SPSi possess 7 nm mesopores, whereas the HMS possesses a smaller mesopore of about 2.5 nm (Table 1). The BET areas follow the order HMS > SBA-15 > SPSi (Table 1). The ^{29}Si MAS and CPMAS NMR of these materials (Fig. 2) clearly show three different Si types: Q^2 , Q^3 and Q^4 . Deconvoluting the first spectra using three Gaussian peaks, a perfect fit is obtained (Fig. S1 of ESI[†]),

centered at -91.5 , -100.9 and -110.1 ppm (Table 1), in agreement with the literature.¹⁹ The amount of Q^2 and Q^3 Si sites due to the silanols $[\text{Si}-(\text{OSi})_2-(\text{OH})_2]$ and $[\text{Si}-(\text{OSi})_3-\text{OH}]$, respectively, is significantly lower than the silica framework Q^4 sites, $[\text{Si}-(\text{OSi})_4]$ (Table 1). Hence all mesoporous silicas possess the essential Q^2 and Q^3 silanols for their surface post-functionalization in the order HMS > SBA-15 > SPSi. This order is the same for the materials surface area and thus the higher the materials surface area the higher the amount of available silanols.

Nevertheless, the amount of surface silanols might be correlated with the acidity, which might influence the course of asymmetric organic transformations and/or the stability of the immobilized homogeneous catalysts. The pH_{pzc} values for SBA-15 and SPSi were 3.5 and 5, respectively, which is in accordance with the amount of silanols on the surface. But for the HMS sample the pH_{pzc} value was 4.1, higher than that for SBA-15 which possesses lower amounts of silanols.

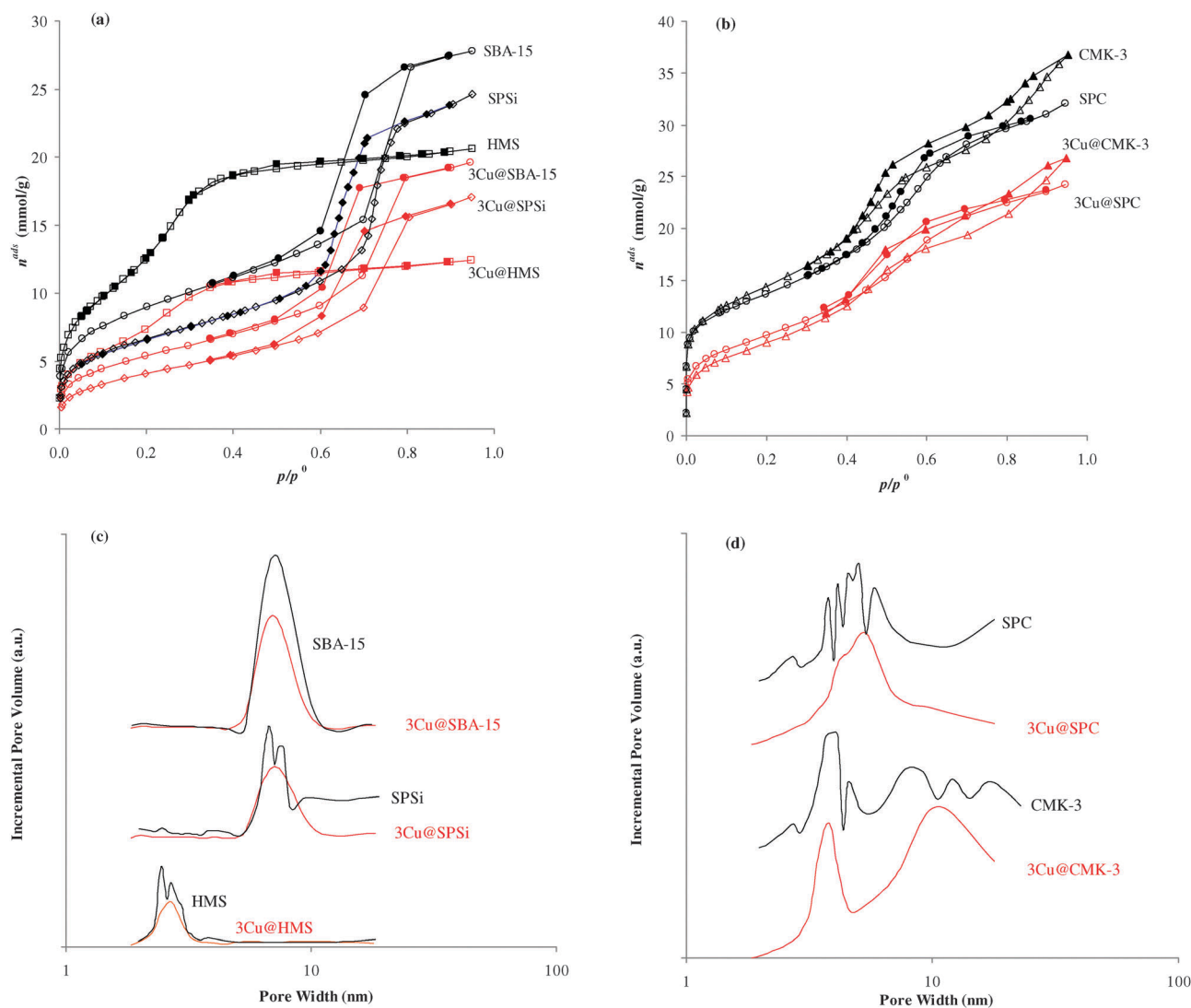
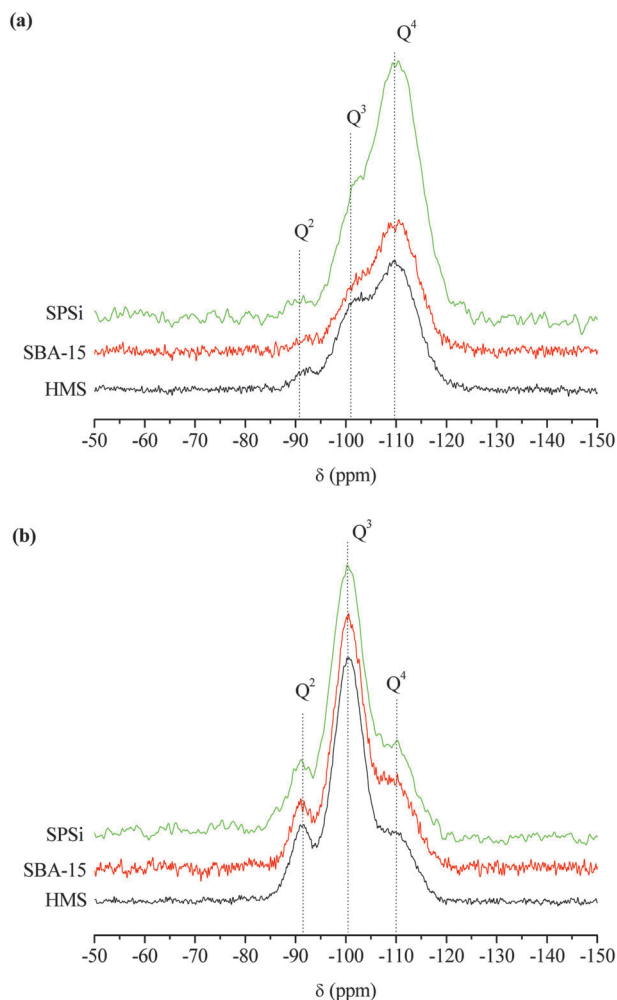


Fig. 1 (a) and (b) Nitrogen adsorption–desorption isotherms, at $-196\text{ }^{\circ}\text{C}$, and mesopore size distributions for the indicated samples (open points adsorption; closed points desorption). (c) and (d) Mesopore size distributions from the BdB method.

Table 1 Deconvolution of the ^{29}Si MAS NMR of the mesoporous silicas,^a pH_{pzc} and textural properties of all the materials

	Q^2		Q^3		Q^4		pH_{pzc}^b	Textural properties		
	% Area	ppm (width)	% Area	ppm (width)	% Area	ppm (width)		$A_{\text{BET}}^c/\text{m}^2 \text{g}^{-1}$	$V_{\text{total}}^d/\text{cm}^3 \text{g}^{-1}$	w^e/nm
HMS	4.5	-91.9 (4.2)	29.4	-101.0 (6.4)	66.1	-110.0 (8.4)	4.1	994	0.72	2.4; 2.7
SBA-15	3.5	-92.0 (4.8)	21.5	-100.9 (6.3)	75.0	-110.1 (8.6)	3.5	756	0.99	7.1
SPSi	2.5	-90.7 (4.6)	18.2	-100.7 (6.1)	79.3	-110.2 (9.1)	5.0	571	0.84	6.6; 7.4
CMK-3							4.7	1396	1.26	4.0; 7.7
SPC							3.3	1140	1.23	3.7–5.8

^a Deconvoluted spectra in Fig. S1 of ESI. ^b pH at which the material has a net zero surface charge. ^c Specific surface area. ^d Total porous volume. ^e Maxima in the widths (w) of the mesopore size distributions for the various samples.

**Fig. 2** Solid state NMR of the mesoporous silicas: (a) ^{29}Si MAS and (b) ^{29}Si CPMAS.

Hence there is no linear correlation between the amount of silanols of mesoporous silicas and their pH_{pzc} . However this result shows that materials with similar pore size, SBA-15 and SPSi, prepared using the same structuring agent, but by different procedures, yield different surface acidities.

These last materials, SBA-15 and SPSi, were also used as templates for the preparation of two carbon mesoporous materials, CMK-3 and SPC, but using different methodologies. Both materials possess higher areas than the parent mesoporous silicas, due to the presence of micropores also, with mesopores

of 4.0 and 7.7 nm for CMK-3 and in the range of 3.7–5.8 for SPC. The pH_{pzc} values are 4.7 and 3.3, for CMK-3 and SPC, respectively. Hence lower surface acidity was obtained for CMK-3 when compared to its parent SBA-15, whereas the SPC possesses higher surface acidity than SPSi. Again by using two different synthesis methodologies two mesoporous carbon materials were obtained with different surface and textural properties.

Composition modified materials. 3-Bromopropyltrimethoxysilane functionalized copper(II) aza-bis(oxazoline) (CuazaBox, **3Cu**) was anchored according to Scheme 2 onto the two ordered mesoporous silicas, SBA-15 and SPSi, their carbon replicas, CMK-3 and SPC, respectively, and a smaller pore mesoporous silica (HMS). The alkoxy groups of the functionalized **3Cu** complex react with the silanol groups at the surface of the mesoporous silicas and the surface phenol groups of the carbon materials, likewise our previous work on the immobilization of homogeneous catalysts onto activated carbons.^{27,28} As described in the experimental section, at the end of the anchoring procedure the materials were extensively washed and refluxed in order to remove the eventual physisorbed catalyst. Thus simple physisorption onto the carbon surface can be ruled out, besides π - π interactions since the azaBox ligand does not present a π system, like the previously explored salen ligands. This is also supported by the fact that the **3Cu**@SPC heterogeneous catalyst did not deactivate upon reuse and this heterogeneous catalyst and **3Cu**@CMK-3 also work with lower homogeneous catalyst densities than in the case of the mesoporous silicas (see Section 3.2).

The elemental analysis of all the materials, compiled in Table 2, shows the presence of nitrogen which indicates that the anchoring of the chiral ligand **3** onto the materials was successful. Taking into consideration that a **3** molecule contains three atoms of nitrogen (Scheme 2), the amount of anchored **3** can be calculated, which is also compiled in Table 2. Hence, the order of the chiral ligand loading is SPSi > SBA-15 \approx CMK3 > SPC > HMS. Although SBA-15 and its carbon replica possess similar amounts of anchored **3**, SPSi has a higher amount of **3** than its carbon replica (SPC). The highest amount of ligand loading found for SPSi is most probably related to the nature of its surface since, as indicated above, the pH_{pzc} values showed that the SPSi material has the least acidic surface. In fact, considering on one hand the silicas and, on the other hand, the replicas, ligand loadings are in general highest for the least acidic materials.

Table 2 Chemical analysis and textural properties of the modified materials

Sample	Elemental analysis				ICP %Cu	$\mu\text{mol g}^{-1}$			Textural properties				Density/ $\mu\text{mol m}^{-2}$	
	%N	%C	%H	%S		3 ^a	OTf ^b	Cu ^c	Cu/3	1/2 × OTf/3	$A_{\text{BET}}^f/\text{m}^2 \text{g}^{-1}$	$V_{\text{total}}^g/\text{cm}^3 \text{g}^{-1}$	Cu	3
3Cu@SBA-15	0.51	3.12	0.90	0.94	1.0	121	293	157	1.3	1.2	438	0.68	0.21	0.16
3Cu@CMK-3	0.50	80.71	1.12	0.94	0.9	119	292	142	1.2	1.2	717	0.94	0.10	0.09
3Cu@SPSi	0.64	3.92	0.70	0.89	1.0	151	278	157	1.0	0.9	339	0.60	0.28	0.26
3Cu@SPC	0.40	79.95	0.74	^d	0.57	94	^e	90	1.0		772	0.85	0.08	0.08
3Cu@HMS	0.35	2.61	1.13	0.78	0.88	83	242	138	1.7	1.5	584	0.44	0.14	0.08

^a Calculated from the EA nitrogen content. ^b Calculated from the EA sulfur content. ^c Calculated from the ICP copper content by using the formula: %Cu × 10⁻⁶/(100 × 63.456). ^d Below the detection limit: 0.30%. ^e Below the detection limit: 94 $\mu\text{mol g}^{-1}$. ^f Specific surface area. ^g Total porous volume.

From the elemental analysis the presence of sulphur which is from the triflate (OTf) counter-anion of copper(II) can also be observed, showing that copper(II) coordination took place. Taking into consideration that each triflate contains one sulphur atom, the amounts of triflate anion can be calculated (Table 2). Thus, the order of the triflate anion content is SBA-15 ≈ CMK-3 > SPSi > HMS. Hence the order of loading of triflate is different from that of ligand 3 suggesting that the amount of copper will also be different from that of 3 and generally slightly higher as can be seen by the 1/2 × OTf/3 ratio, also compiled in Table 2.

To confirm this, the copper content of the materials was also obtained by ICP-AES in order to determine the amount of copper coordinated to ligand 3. As can be seen in Table 2, the amounts of copper are higher than those of 3 from the Cu/3 ratio, for 3Cu@SBA-15, 3Cu@CMK-3 and 3Cu@HMS, which are similar to the 1/2 × OTf/3 ratio, indicating that the copper content can be roughly determined through its counter-anion. However the order of copper loading onto the materials is slightly different from that of the OTf anion: SBA-15 = SPSi > CMK-3 > HMS > SPC. The ordered mesoporous silicas (SBA-15 and SPSi) possess more copper than their corresponding carbon replicas (CMK-3 and SPC).

XPS. For some of the heterogeneous catalysts prepared, for which enough sample was available, XPS was also performed: 3Cu@SBA-15, 3Cu@HMS and 3Cu@SPC. Besides of a large amount of silica and oxygen, and carbon in the case of the 3Cu@SPC material, copper, sulphur and fluorine were detected at the surface of these materials indicating the presence of copper(II) triflate, as well as nitrogen showing the presence of the chiral ligand 3 (Table S1, ESI[†]).

The N 1s peaks of the materials are centered between 399.6 and 400.8 eV and are large indicating the presence of the chiral ligand 3 with imine nitrogen^{29,30} as well as tertiary amine (Table S2, ESI[†]). The Cu 2p_{3/2} peaks are centered between 932.8 and 934.2 eV, which are typical of copper(II) complexes in a mixed N,O coordination sphere.^{29–31} However for the SPC materials the Cu 2p_{3/2} peak is larger and higher in energy than for the other two analyzed silica materials. The O 1s spectra of 3Cu@SBA-15 and 3Cu@HMS can be deconvoluted into a single peak centered at 532.8 eV, whereas the one for 3Cu@SPC is larger and can be deconvoluted into 3 peaks at 531.8, 533.7 and 536.8 eV (Table S2, ESI[†]). Thus the O 1s XPS spectra of the

mesoporous silicas are typical of the Si–O bonds of the framework, whereas a rich oxygen surface chemistry can be deduced for the SPC material.³² This last conclusion is supported by the lowest pH_{pzc} value observed for the SPC mesoporous carbon (Table 1). Although the signal to noise of the Cu 2p spectra of 3Cu@SPC is low, the higher energy and peak width observed for Cu 2p_{3/2} of 3Cu@SPC suggests that there must be copper(II) in different environments, when compared to 3Cu@SBA-15 and 3Cu@HMS. In the C 1s high resolution spectra besides the bands due to the carbon backbone of oxazoline and the propyl linker at lower energy, for the 3Cu@SBA-15 which contains a higher surface amount of copper, a band at 292 eV due to the CF₃ carbon of the triflate anion can be clearly observed (Table S2, ESI[†]). This anion also gives rise to an intense peak in the F 1s region, with a band at 688 eV (Table S2, ESI[†]), whereas sulphonate sulfur can sometimes be detected at 168 eV (Table S2, ESI[†]).

FTIR. The FTIR spectra of the mesoporous silica materials, SBA-15, SPSi and HMS, are dominated by the Si–O asymmetric and symmetric stretching vibrations, respectively, at 1050 and 800 cm⁻¹ (Fig. 3). Moreover by ATR a low intensity peak at 3746 cm⁻¹ can be distinguished in the spectra of these materials, which is due to the stretching of the O–H groups from the isolated silanols (Si–OH).³³ Although the samples were dried for 6 hours at 100 °C under vacuum, O–H stretching and bending vibrations around 3450 and 1640 cm⁻¹, respectively, from adsorbed water can still be observed. The carbon mesoporous materials, CMK-3 and SPC, show very low intensity broad bands also around 3500 and 1639 cm⁻¹ which may be due to the O–H stretching and bending vibrations, respectively, of adsorbed water, as well as a broad band at 1100 cm⁻¹ probably due to the Si–O stretching vibration of the remaining silica templates.

In the materials containing the anchored 3Cu, represented in Fig. 3, besides the characteristic bands of the materials very low intensity bands at 2976, between 1560 and 1360 and about 640 cm⁻¹ due, respectively, to the C–H stretching vibrations of the 3 *tert*-butyl groups, vibrations characteristic of ligand 3 and S=O vibration of the sulfonate group of the triflate counter anion of the copper(II) can be further seen (Fig. 3f and Scheme 2). The characteristic C=N stretching vibration of ligand 3 (Fig. 3f and Scheme 2) can be clearly seen in the ATR spectra at 1619 cm⁻¹, but some extent of superimposition

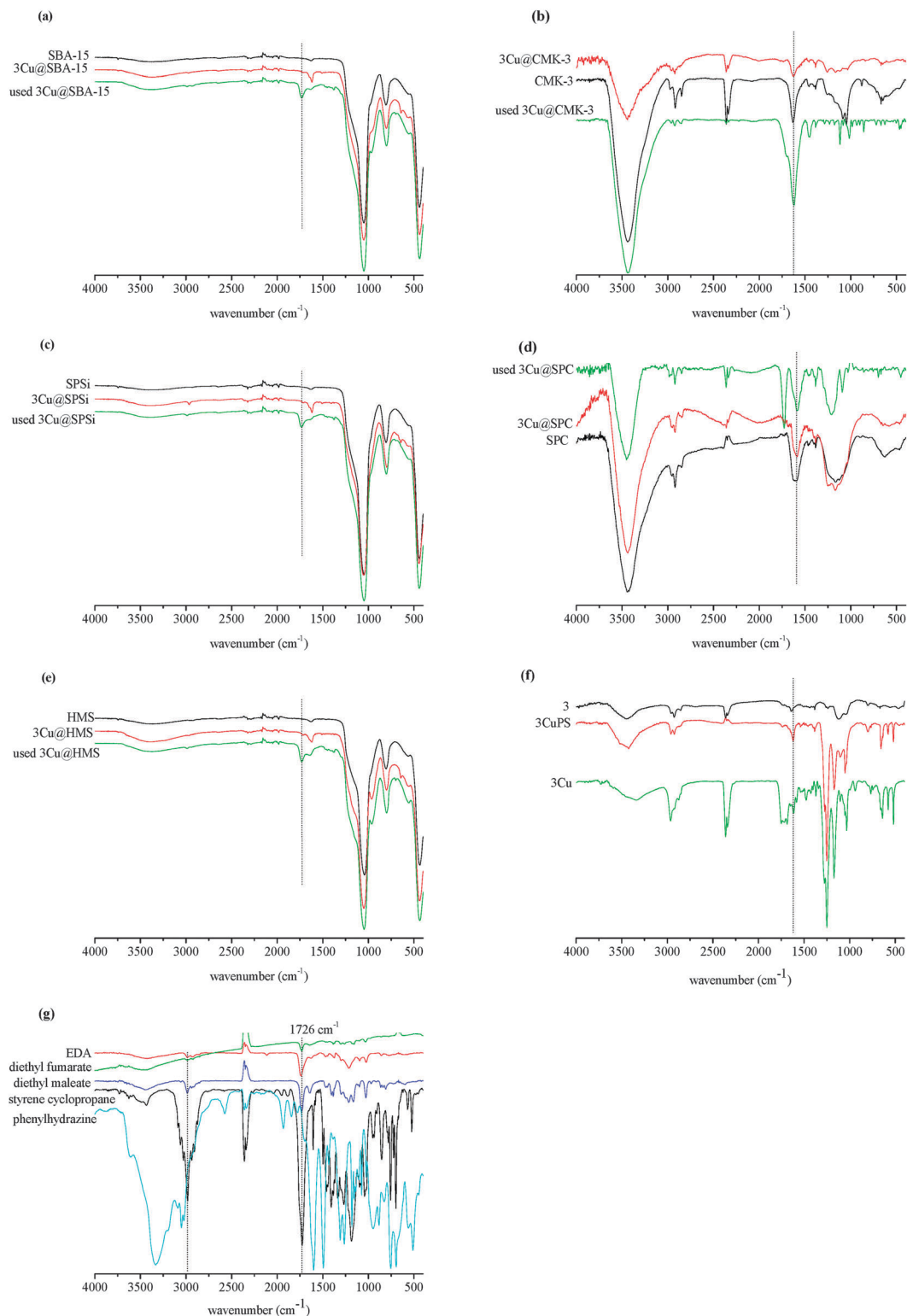
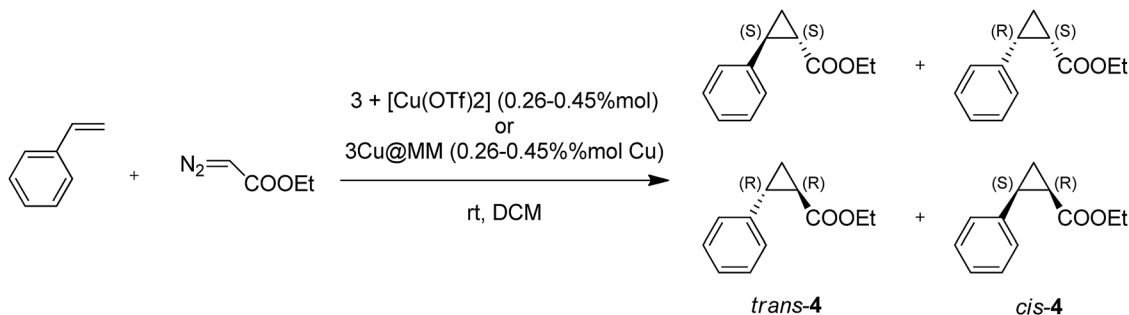


Fig. 3 FTIR spectra for the mesoporous materials (MM) and **3Cu@MM** materials, before and after catalysis: (a) SBA-15, (b) CMK-3, (c) SPSi, (d) SPC and (e) HMS, (f) azaBox (**3**), CuazaBox (**3Cu**) and CuazaBoxPS (**3CuPS**) and (g) EDA, styrene cyclopropane, diethyl fumarate and diethyl maleate.

of the O–H bending vibration at 1637 cm^{-1} of the water adsorbed on the surface of the materials can also be observed. Furthermore the low intensity band at 3746 cm^{-1} , due to the stretching of the O–H groups from the isolated silanols, disappeared

confirming that grafting between this group and the propylsilane functionalized **3Cu** took place according to Scheme 2.³³

It is worth mentioning that copper(II) coordination to the functionalized ligand **3** can be detected as shown in Fig. 3f by



Scheme 3 Cyclopropanation of styrene with ethyldiazoacetate.

the shift of the C=N stretching band from 1641 cm^{-1} in ligand **3** to 1620 cm^{-1} in the functionalized ligand **3**, before addition of the materials to the reaction mixture (see Section 2.4 and Scheme 3).

Thermogravimetry with differential scanning calorimetry.

The TG-DSC results obtained in an oxidizing atmosphere are usually more informative than those obtained in an inert atmosphere but, to avoid the decomposition of the matrix, in the case of carbon replicas an inert atmosphere was used. By comparing the curves (Fig. 4), for the same material, before and after functionalization, the weight loss up to $250\text{ }^{\circ}\text{C}$, and the corresponding endothermic broad DSC peak, is ascribed mainly to water loss. The transformations above $250\text{ }^{\circ}\text{C}$ can be identified with the decomposition of the **3Cu** complex. For the carbon replicas the progressive fall of the weight curve, and the lack of clear transformation in the DSC curve, makes the interpretation difficult. For the silicas, the pattern is much similar for both, SBA-15 and HMS with a weight loss between $250\text{ }^{\circ}\text{C}$ and $415\text{ }^{\circ}\text{C}$ associated to an exothermic transformation, both compatible with the decomposition of the complex by thermal oxidation. In the case of the SPSi sample the DSC exothermic transformation extends until higher temperatures ($450\text{ }^{\circ}\text{C}$), than for the other silicas, and presents a more well defined peak. We attribute this enhanced definition in the DSC peak to a more uniform distribution of the complex in the matrix, in relation to the other silicas, which is also in line with the least acidity of the SPSi sample, as mentioned above in the discussion of the pH_{pzc} values. In fact, being a less acidic material, a more homogeneous reactivity of the surface silanol groups could be expected.

Nitrogen adsorption at $-196\text{ }^{\circ}\text{C}$. Fig. 1 displays the nitrogen adsorption-desorption isotherms at $-196\text{ }^{\circ}\text{C}$, of the materials before and after functionalization with **3Cu**, and the respective mesopore size distributions estimated from the Broekhoff-de Boer method, in a version simplified with the Frenkel-Halsey-Hill equation (BdB-FHH).³⁴ The general pattern of reduction in the porous volume and specific surface areas (Tables 1 and 2) after functionalization, already mentioned in the literature for other systems, is noticed.^{18,19} In the case of the silica materials, most probably because the mesopore size distributions are much more uniform in relation to the carbon replicas (Fig. 1c and d), the shape of the distribution is, essentially, kept. For the carbon replicas, the main changes occur for the CMK-3

samples where a relative inversion on the heights of the maxima near 4 and near 7.7–10 nm seems to occur after functionalization with the **3Cu** complex. CMK-3 also presents the highest decrease in the porous volume.

3.2. Catalysis experiments

The copper(II) complexes with aza-bis(oxazoline) ligands are efficient homogeneous catalysts in the asymmetric cyclopropanation of alkenes.^{3,4,21,22} Therefore, the nanostructured materials with anchored **3Cu** were tested as heterogeneous catalysts in the asymmetric cyclopropanation of styrene with ethyldiazoacetate at room temperature (Scheme 3) and the results are compiled in Table 3.

Catalytic activity, diastereoselectivity and enantioselectivity.

From Table 3 (please also see Scheme 3 for the nomenclature of reaction products) it can be seen that all the materials are active in the asymmetric cyclopropanation of styrene with high *trans*-**4** diastereoselectivity (70–72%) and moderate to high enantioselectivities. The order of the values for this last parameter is SPSi (72% *cis*-**4** and 80% *trans*-**4**) > CMK-3 (70% *cis*-**4** and 79% *trans*-**4**) > SPC (63% *cis*-**4** and 75% *trans*-**4**) > SBA-15 (62% *cis*-**4** and 72% *trans*-**4**) \gg HMS (36% *cis*-**4** and 47% *trans*-**4**). Hence the ordered mesoporous silica SPSi gives rise to the most enantioselective heterogeneous catalyst. Moreover, as can be seen in Table 3, the enantioselectivities of the heterogeneous catalysts are much higher than the corresponding homogeneous phase reactions run under the same experimental conditions and using the same amount of Cu (0.46 or 0.26% mol, Table 3), with the only exception of **3Cu**@HMS. Therefore positive effects on the enantioselection of the **3Cu** catalyst can be observed upon immobilization for all the materials used, probably due to the introduction of the propyl groups on the acidic **3** nitrogen (Scheme 2). In fact, higher enantioselectivities were reported for methylated **3** and thus propylation of **3** should also increase its enantioselectivity as observed herein.³ Taking into consideration only the silica mesoporous materials, it is curious to note that the SBA-15 material gives rise to a less enantioselective heterogeneous catalyst than using SPSi as a support, despite the similarity of the textural properties of both materials. The least enantioselective heterogeneous catalyst was nevertheless when the HMS material was used as the support, indicating that a smaller pore size is not beneficial to the course of the asymmetric cyclopropanation

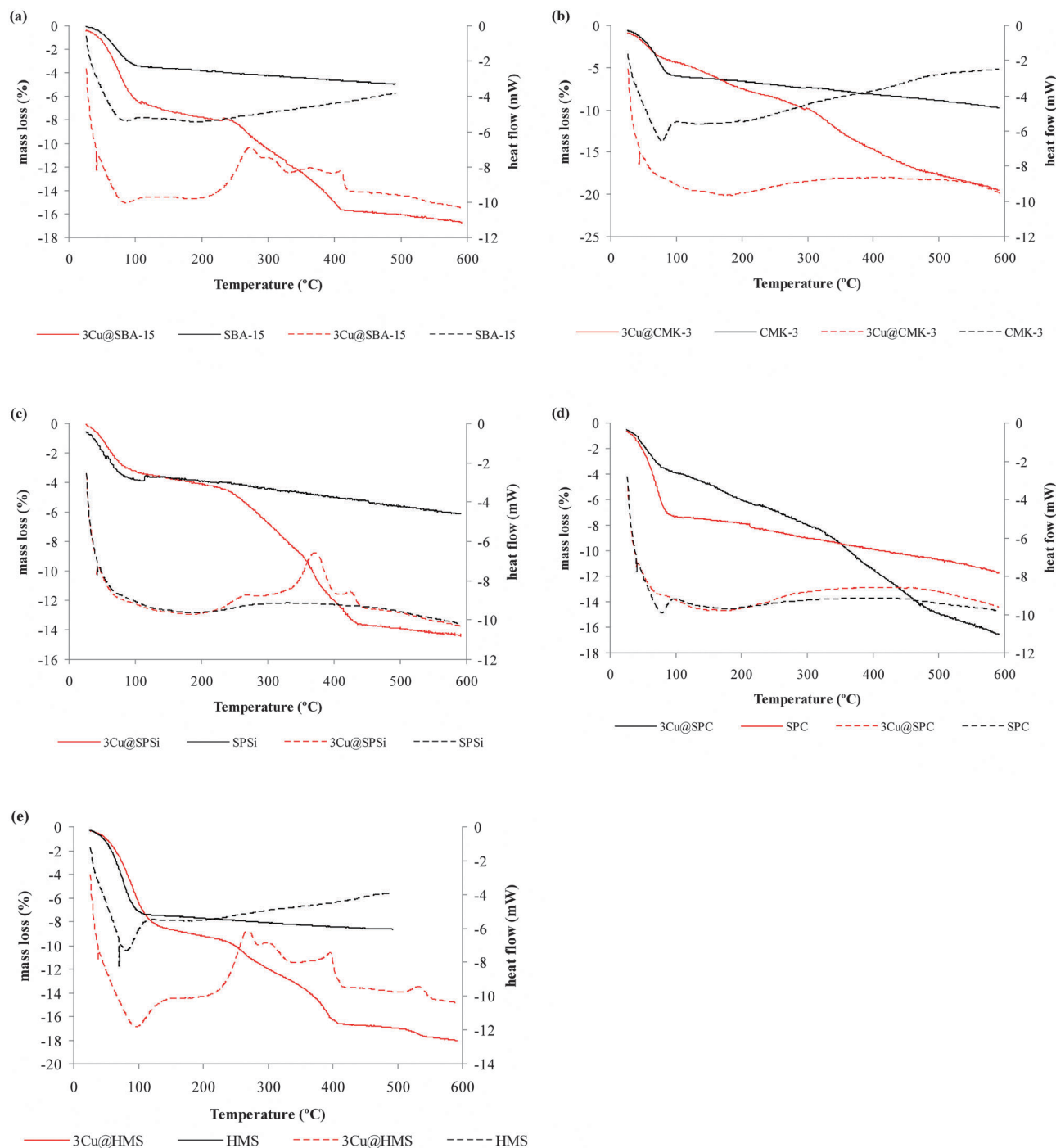


Fig. 4 Thermogravimetric curves for the various samples (a) SBA-15, (b) CMK-3, (c) SPSi, (d) SPC, (e) HMS.

of styrene. Nonetheless, this last material has lower amounts of copper and **3** than the other mesoporous silicas, besides the highest Cu/**3** ratio, which can also partially justify the lowered performance compared with the other materials. For the other heterogeneous catalysts with a slightly higher content of copper than ligand it does not seem to be a very important factor, as **3Cu@CMK-3** presents comparable enantioselectivity as **3Cu@SPSi**, with the same amount of copper and ligand.

The catalyst densities for both Cu and azaBox were also calculated and can be found in Table 3. However the catalyst density and type of material could not explain the differences observed for the enantioselectivity of the several heterogeneous catalysts. The catalytic performance in the first cycle of **3Cu@CMK-3** with $0.1 \mu\text{mol m}^{-2}$ is comparable to the best catalyst **3Cu@SPSi** with the highest density of $0.3 \mu\text{mol m}^{-2}$. Comparing **3Cu@CMK-3** and **3Cu@SPC**, both with $0.1 \mu\text{mol m}^{-2}$ of active phase, the first is found to be a better heterogeneous

Table 3 Cyclopropanation of styrene with azaBox ligand immobilized onto various porous supports and in a homogeneous phase^a

Catalyst	t/h	Run	mol% ^b		%C ^c	4 <i>trans/cis</i> ^d	%ee (4) ^e		TON ^f
			Cu	3			<i>cis</i>	<i>trans</i>	
3 + [Cu(OTf) ₂]	24	1st	0.27	0.26	19	66/34	41	44	70
3 + [Cu(OTf) ₂]	24	1st	0.46	0.48	42	73/27	63	73	90
3 + [Cu(OTf) ₂]	3	1st	1.0	1.0	56	73/27	76	84	56
3Cu@SBA-15	24	1st	0.46	0.35	22	70/30	62	72	47
	24	2nd	0.36	0.28	15	65/35	41	51	43
3Cu@CMK-3	24	1st	0.37	0.32	47	72/28	70	79	126
	24	2nd	0.37	0.31	39	65/35	38	45	104
3Cu@SPSi	24	1st	0.45	0.43	53	71/29	72	80	118
	24	2nd	0.40	0.38	26	70/30	64	72	65
3Cu@SPC	24	1st	0.26	0.27	37	70/30	63	75	130
	24	2nd	0.26	0.27	41	67/33	52	59	158
3Cu@HMS	24	1st	0.40	0.24	51	70/30	36	47	125
	24	2nd	0.38	0.23	10	64/36	40	49	28

^a Reactions performed at room temperature using 2.40 mmol styrene, 0.65 mmol *n*-undecane (internal standard), 70 mg of heterogeneous catalyst, 2 μ L phenylhydrazine and 2.75 mmol of EDA in 10.0 mL of CH₂Cl₂. ^b % of copper and 3 in the catalyst in relation to styrene (see Table 1); for the recycling experiments corrected for the loss of heterogeneous catalyst weight. ^c Conversion of styrene determined by GC-FID. ^d *trans/cis* ratio of 4 (Scheme 3). ^e *cis* and *trans* 4 (Scheme 3) enantiomeric excesses determined by chiral GC-FID. ^f TON = moles of styrene converted/moles of Cu.

catalyst than the second. Nevertheless, in the case of the mesoporous silicas the catalyst density might be an important factor as 3Cu@SPSi, with 0.3 μ mol m⁻² of active phase, presents better enantioselectivity than 3Cu@SBA-15 (0.2 μ mol m⁻²) and 3Cu@HMS (0.1 μ mol m⁻²). Hence we were driven to search for another support property that could explain the different enantioselectivities observed between all the heterogeneous catalysts. It is difficult to correlate the results from enantioselectivity with the textural and surface chemistry properties of the materials. Nevertheless an attempt can be made for instance considering the SBA-15 and the SPSi samples. For these samples the mesopore size distributions are comparable, although the porous volume of SBA-15 is 18% higher (Table 1). Therefore, the most important parameter in this case seems to be the surface chemistry since, as discussed above, the SPSi surface is less acidic than the one of SBA-15 allowing as well a more uniform distribution of the complex in the SPSi matrix, as suggested earlier by the DSC results (Fig. 4). Moreover, the SPSi carbon replica (SPC) yields a least enantioselective heterogeneous catalyst, whereas CMK-3 yields a more enantioselective heterogeneous catalyst than SBA-15. Despite the differences in the framework composition, textural and surface chemistry properties the same dependence on surface acidity can be inferred. SPC presents a more acidic surface than its parent SPSi and lower enantioselectivities were obtained, whereas the lower acidity of the CMK-3 surface yields a more enantioselective heterogeneous catalyst than its parent SBA-15 (Tables 1 and 3). It is also clear from the results in this work that small mesopore sizes, in the range of those presented by the HMS material, might be disadvantageous in the present context since this solid presented the lowest chiral ligand loading and the lowest enantioselectivity values.

It is noteworthy that in our previous report, upon heterogenization of 2Cu (Scheme 1) onto mesoporous silicas and their carbon replicas, the SPSi material also led to the heterogeneous catalyst with the highest enantioselectivity.²⁰ Therefore this

material seems to be superior as a support than conventional SBA-15, and their carbon replicas.

On the other hand, immobilization of the 3Cu catalyst on these mesoporous silica materials also leads to better styrene conversions and TON than the corresponding homogeneous phase reactions (0.46 or 0.26 mol%, Table 3). Therefore positive effects on the catalytic activity of the 3Cu catalyst can also be observed upon immobilization for these silica materials, probably due to the introduction of the propyl groups on the acidic 3 nitrogen (Scheme 2).³ The order for the styrene conversions is SPSi (53%) > HMS (51%) > CMK-3 (47%) > SPC (34%) > SBA-15 (22%). These values do not follow the materials' copper contents (Table 2, see Section 3.1.1). The SPSi and HMS mesoporous silicas were the ones which convert more styrene followed by the mesoporous carbons and finally SBA-15. The TON of the heterogeneous phase reactions are high and in the order: SPC (130) > CMK-3 (126) \approx HMS (125) > SPSi (118) \gg SBA-15 (47). It can be concluded that the ordered mesoporous carbons, SPC and CMK-3, yield more active heterogeneous catalysts than when the corresponding mesoporous silicas are used as 3Cu catalyst supports. This is the opposite of that observed for the heterogenized 2Cu on the same supports²⁰ and could be due to a different effect of the type of matrix support, *i.e.* carbon *vs.* silica on the heterogenized homogeneous catalyst. Since the heterogeneous catalyst with the HMS material as a support, bearing a pore size near to 2.5 nm,^{19,20} has a comparable TON as the ones with the mesoporous carbon materials, their higher activity can also be due to the pore size of the materials, since they possess a pore size of 4.0 nm, whereas their parent ordered mesoporous silicas possess pore sizes of around 7 nm.²⁰ The rate determining step in the cyclopropanation of styrene with copper bis(oxazoline) ligands is the formation of a copper(i) carbene complex by coordination of ethyl diazoacetate to the copper centre.^{10,31} By influence of the spatial restrictions the change in the orientation of the reacting alkene with respect to the catalytic center on the surface of the material, the activity of the system will change,

as in the case of enzymes. In smaller pores the trajectory of the reacting alkene might be shorter and directed by the constraints imposed by the pore, yielding therefore an improved activity.

3Cu immobilized onto siliceous mesocellular foam (MCF) using the same anchoring procedure as the one reported herein gave 75% yield of cyclopropane, 86% ee for the *trans* and 78% ee for the *cis* cyclopropane with a diastereoselectivity of 62% *trans* to 38% of *cis*.²¹ The enantioselectivities are comparable to our best heterogeneous catalyst, **3Cu@SPSi**, but the yields are higher probably because this reaction was performed in an inert atmosphere and using an excess of styrene in relation to EDA. The reported diastereoselectivity is however lower. Nevertheless, by capping the surface silanols of the MCF Ying *et al.* could further increase the cyclopropane yield and enantioselectivity to 69 and 88% ee for the *trans* and 83% ee for *cis*.²¹ **3Cu** has also been immobilized onto a polymeric support^{3,22,35} methoxypolyethylene glycol and polystyrene; using the first polymer in the cyclopropanation of styrene but with methyl diazoacetate gave 69% yield of cyclopropanes, with 71% *trans* to 29% *cis* cyclopropane diastereoselectivity and 91 and 87% enantioselectivity, respectively;³ whereas with polystyrene and again methyl diazoacetate, 28% yield, 70% *trans* to 30% *cis* cyclopropane and 88% *trans* enantioselectivity was obtained.^{22,35} The enantioselectivities and diastereoselectivities are comparable to our best heterogeneous catalyst, **3Cu@SPSi**. Hence a hydrophobic surface seems to be an important factor in designing new robust materials for being used as supports in asymmetric catalysis. On the other hand, **3Cu** immobilized onto a Laponite clay and a Nafion silica through electrostatic interactions showed slightly higher enantioselectivities (76% *cis*, 83% *trans* and 81% *cis*, 88% *trans*, respectively), but lower yields (46 and 30%, respectively) than our best heterogeneous catalyst, **3Cu@SPSi**, under comparable experimental conditions.⁴ Also in comparison with our previous reports on the immobilization of commercial bis(oxazoline) catalysts, **1Cu**^{18,19} and **2Cu**²⁰ (Scheme 1), better enantioselectivities and styrene conversions were generally achieved herein with the **3Cu** catalysts indicating that their copper(II) complexes must be more stable than with the former homogeneous catalysts, as described in the literature.⁴

It is noteworthy that in the present reaction no by-products other than diethyl fumarate and diethyl maleate, which are from the dimerization of EDA, were detected. Hence the styrene conversions can be taken as the yields of cyclopropanes.

Recycling. The main aim of the immobilization of homogeneous catalysts is its easy separation from the reaction media, at the end of the reaction, and the possibility of further use in more catalytic cycles. Besides that, it is well known that single site isolation of homogeneous catalysts onto a porous material may increase its stability. Hence the composite materials were reused in more successive catalytic cycles after filtration from the solution, washing with dichloromethane and drying. The results are also compiled in Table 3. It can be concluded that they can be reused with comparable enantioselectivities, for HMS and SPSi, and decrease in the

enantioselectivity for the other heterogeneous catalysts. Higher decreases in enantioselectivity can be observed for the heterogeneous catalysts with SBA-15 and CMK-3. With the exception of **3Cu@SPC** there is loss of activity upon reuse, which may indicate that although the stability of the copper(II) complexes with **3** is higher than those of commercial bis(oxazoline), **1Cu**^{18,19} and **2Cu**,²⁰ there is still some degree of instability of the chiral complex or partial deactivation of the immobilized **3Cu** complex. The FTIR spectra of the materials at the end of the recycling experiments (Fig. 3) show a very intense band at 1726 cm⁻¹, which is typical of the carbonyl in the ester group,³⁵ as can be confirmed from Fig. 3g, representing the spectra of the reagent EDA and products styrene cyclopropane and by-products diethyl fumarate and diethyl maleate. The vibration of the carbonyl band in the recycled heterogeneous catalysts is closer to that of the styrene cyclopropane and diethyl maleate and diethyl fumarate by-products, formed from EDA dimerization. Therefore, as observed by us previously in the presence of more nitrogen and carbon (EA) on recycled catalysts,¹⁸ strong adsorption of by-products cannot be ruled out as it would also justify the lowering of the catalytic activity of the heterogenized catalysts.³⁶

Nonetheless, the heterogeneous catalysts using the carbon materials as supports remain quite active upon reuse, when compared with the mesoporous silicas, and the SPC retains most of its enantioselectivity upon reuse.

Deactivation upon reuse was also observed for **3Cu** immobilized onto a Laponite clay and a Nafion silica through electrostatic interactions,⁴ as well as polystyrene.²² It is also commonly observed for commercial bis(oxazoline) catalysts immobilized onto mesoporous silica materials.^{19,20,37} Only when immobilized onto siliceous mesocellular foam,²¹ which possesses ultra-large pores of 25 nm, and methoxypolyethylene glycol³ that these systems present high enantioselective activity and recyclability. It is noteworthy, however, that the catalytic studies on these reports were performed using 1–2 mol% of Cu^{21,22} in relation to the substrate, double than the necessary in homogeneous phase reactions,² whereas in our catalytic experiments the Cu and azaBox contents were between 0.26–0.51 and 0.11–0.43 mol%, respectively. Thus deactivation is more difficult to detect than in our case.

4. Conclusions

A copper(II) chiral aza-bis(oxazoline) homogeneous catalyst (**3Cu**) could be anchored onto ordered silica mesoporous materials and their carbon replicas. The materials pH_{pzc} proved to be an important factor in the **3Cu** anchoring yields, as well as in the uniform distribution of the complex in the SPSi matrix. All the composites prepared were more active and enantioselective in the cyclopropanation of styrene than in the corresponding homogeneous phase reactions, run under the same experimental conditions, suggesting positive immobilization effects, with the only exception of **3Cu@HMS** that presented lower enantioselectivity. The most enantioselective heterogeneous catalyst, with %ee *cis* and %ee *trans* of 72 and 80,

respectively, was the one using the ordered mesoporous silica SPSi. Since CMK-3 was the second most enantioselective catalyst with %ee *cis* and %ee *trans* of 70 and 79, surface chemistry seems to be an important parameter as these two materials present the highest pH_{pzc} values of the studied supports. The ordered mesoporous carbons, CMK-3 and SPC, yield higher reaction TON than when the parent mesoporous silicas, SBA-15 and SPSi, are used as catalyst supports. This could be due to the pore size of the materials as the HMS material, with a pore size much smaller than SBA-15 and SPSi, is also a very active catalyst.

The heterogeneous catalysts with HMS, SPSi and SPC can be reused with comparable enantioselectivities, or decrease in the enantioselectivity, and with higher activity in the case of the SPC. But for most of the catalysts there is loss of activity upon reuse which could be due to partial deactivation, probably by coordination of the EDA dimerization by-products.³⁶

The results presented herein are comparable to the ones of the same 3Cu homogeneous catalyst immobilized onto mesoporous foams,²¹ despite different experimental conditions, and superior to the same catalysts immobilized by electrostatic interactions into clays.⁴

Herein, with this comprehensive study, we were able to show that when preparing asymmetric heterogeneous catalysts the acidity of the support surfaces can have a detrimental role on the enantioselection of the immobilized chiral homogeneous catalyst. Therefore the preparation of new robust porous materials bearing less acidic surfaces is needed in order to design superior asymmetric heterogeneous catalysts, without the need for post-hydrophobization of the surface.

Acknowledgements

This work was funded by Fundação para a Ciência e a Tecnologia (FCT) through the project PTDC/QUI/64770/2006, which was co-financed by EU under the programs COMPETE, QREN and FEDER. FCT is also acknowledged for financing under the Projetos Estratégicos Pest-C/CTM/LA0011/2011 (CICECO) and PEst-OE/QUI/UI0612/2011 (CQB/FC/UL). ARS thanks FCT, Fundo Social Europeu and Programa Operacional Potencial Humano for the contract under the program Ciência 2008.

References

- H. Pellissier, *Tetrahedron*, 2008, **64**, 7041–7095.
- D. A. Evans, K. A. Woerpel, M. M. Hinman and M. M. Faul, *J. Am. Chem. Soc.*, 1991, **113**, 726–728.
- M. Glos and O. Reiser, *Org. Lett.*, 2000, **2**, 2045–2048.
- J. M. Fraile, J. I. Garcia, C. I. Herrerias, J. A. Mayoral, O. Reiser, A. Socuellamos and H. Werner, *Chem.-Eur. J.*, 2004, **10**, 2997–3005.
- D. A. Evans, M. M. Faul, M. T. Bilodeau, B. A. Anderson and D. M. Barnes, *J. Am. Chem. Soc.*, 1993, **115**, 5328–5329.
- D. A. Evans, S. J. Miller and T. Lectka, *J. Am. Chem. Soc.*, 1993, **115**, 6460–6461.
- D. A. Evans, D. Seidel, M. Rueping, H. W. Lam, J. T. Shaw and C. W. Downey, *J. Am. Chem. Soc.*, 2003, **125**, 12692–12693.
- G. Desimoni, G. Faita and K. A. Jorgensen, *Chem. Rev.*, 2011, **111**, PR284–PR437.
- H. Werner, R. Vicha, A. Gissibl and O. Reiser, *J. Org. Chem.*, 2003, **68**, 10166–10168.
- A. F. Trindade, P. M. P. Gois and C. A. M. Afonso, *Chem. Rev.*, 2009, **109**, 418–514.
- D. Rechavi and M. Lemaire, *Chem. Rev.*, 2002, **102**, 3467–3493.
- J. M. Fraile, J. I. Garcia, C. I. Herrerias, J. A. Mayoral and E. Pires, *Chem. Soc. Rev.*, 2009, **38**, 695–706.
- J. M. Fraile, J. I. Garcia and J. A. Mayoral, *Chem. Rev.*, 2009, **109**, 360–417.
- A. Taguchi and F. Schuth, *Microporous Mesoporous Mater.*, 2005, **77**, 1–45.
- J. Pires, S. Borges, A. P. Carvalho and A. R. Silva, *Adsorpt. Sci. Technol.*, 2010, **28**, 717–726.
- R. Ryoo, S. H. Joo and S. Jun, *J. Phys. Chem. B*, 1999, **103**, 7743–7746.
- C.-C. Ting, H.-Y. Wu, S. Vetrivel, D. Saikia, Y.-C. Pan, G. T. K. Fey and H.-M. Kao, *Microporous Mesoporous Mater.*, 2010, **128**, 1–11.
- A. R. Silva, H. Albuquerque, A. Fontes, S. Borges, A. Martins, A. P. Carvalho and J. Pires, *Ind. Eng. Chem. Res.*, 2011, **50**, 11495–11501.
- A. R. Silva, H. Albuquerque, S. Borges, R. Siegel, L. Mafra, A. P. Carvalho and J. Pires, *Microporous Mesoporous Mater.*, 2012, **158**, 26–38.
- A. R. Silva, L. Carneiro, A. P. Carvalho and J. Pires, unpublished results.
- J. Lim, S. N. Riduan, S. S. Lee and J. Y. Ying, *Adv. Synth. Catal.*, 2008, **350**, 1295–1308.
- H. Werner, C. I. Herrerias, M. Glos, A. Gissibl, J. M. Fraile, I. Perez, J. A. Mayoral and O. Reiser, *Adv. Synth. Catal.*, 2006, **348**, 125–132.
- J. Pires, M. Pinto, J. Estella and J. C. Echeverria, *J. Colloid Interface Sci.*, 2008, **317**, 206–213.
- V. K. Saini, M. Andrade, M. L. Pinto, A. P. Carvalho and J. Pires, *Sep. Purif. Technol.*, 2010, **75**, 366–376.
- P. T. Tanev and T. J. Pinnavaia, *Science*, 1995, **267**, 865–867.
- J. S. Noh and J. A. Schwarz, *J. Colloid Interface Sci.*, 1989, **130**, 157–164.
- B. Jarrais, A. R. Silva and C. Freire, *Eur. J. Inorg. Chem.*, 2005, 4582–4589.
- A. R. Silva, V. Budarin, J. H. Clark, C. Freire and B. de Castro, *Carbon*, 2007, **45**, 1951–1964.
- A. P. Carvalho, C. Castanheira, B. Cardoso, J. Pires, A. R. Silva, C. Freire, B. de Castro and M. B. de Carvalho, *J. Mater. Chem.*, 2004, **14**, 374–379.
- C. Pereira, S. Patricio, A. R. Silva, A. L. Magalhaes, A. P. Carvalho, J. Pires and C. Freire, *J. Colloid Interface Sci.*, 2007, **316**, 570–579.
- J. Pires, J. Francisco, A. Carvalho, M. B. de Carvalho, A. R. Silva, C. Freire and B. de Castro, *Langmuir*, 2004, **20**, 2861–2866.

- 32 J. L. Figueiredo, M. F. R. Pereira, M. M. A. Freitas and J. J. M. Órfão, *Carbon*, 1999, **37**, 1379–1389.
- 33 A. R. Silva, K. Wilson, A. C. Whitwood, J. H. Clark and C. Freire, *Eur. J. Inorg. Chem.*, 2006, 1275–1283.
- 34 W. W. Lukens Jr., P. Schmidt-Winkel, D. Y. Zhao, J. L. Feng and G. D. Stucky, *Langmuir*, 1999, **15**, 5403–5409.
- 35 J. M. Fraile, L. Perez, J. A. Mayoral and O. Reiser, *Adv. Synth. Catal.*, 2006, **348**, 1680–1688.
- 36 S. S. Lee and J. Y. Ying, *J. Mol. Catal. A: Chem.*, 2006, **256**, 219–224.
- 37 J. M. Fraile, J. I. Garcia, C. I. Herrerias, J. A. Mayoral, E. Pires and L. Salvatella, *Catal. Today*, 2009, **140**, 44–50.